Microscopy AND
Microanalysis

Original Article

Microscopic Findings in the Cardiac Muscle of Stranded Extreme Deep-Diving Cuvier's Beaked Whales (*Ziphius cavirostris*)

Nakita Câmara[1,2,3] (iD), Antonio Fernández[1]* (iD), Pedro Herráez[1] (iD), Manuel Arbelo[1] (iD), Marisa Andrada[1] (iD), Cristian M. Suárez-Santana[1] (iD) and Eva Sierra[1] (iD)

[1]Veterinary Histology and Pathology, Institute of Animal Health and Food Safety (IUSA), Veterinary School, University of Las Palmas of Gran Canaria, Campus Universitario Cardones de Arucas, Trasmontaña s/n, Arucas, Las Palmas, Gran Canaria 35413, Spain; [2]Plataforma Oceánica de Canarias (PLOCAN), Carretera de Taliarte s/n, Telde, Las Palmas, Gran Canaria 35214, Spain and [3]Loro Parque Foundation, Avenida Loro Parque s/n, Puerto de la Cruz, Tenerife 38400, Spain

Abstract

Considerable information has been gained over the last few decades on several disease processes afflicting free-ranging cetaceans from a pathologist's point of view. Nonetheless, there is still a dearth of studies on the hearts of these species. For this reason, we aimed to improve our understanding of cardiac histological lesions occurring in free-ranging stranded cetaceans and, more specifically, in deep-diving Cuvier's beaked whales. The primary cardiac lesions that have been described include vascular changes, such as congestion, edema, hemorrhage, leukocytosis, and intravascular coagulation; acute degenerative changes, which consist of contraction band necrosis, wavy fibers, cytoplasmic hypereosinophilia, and perinuclear vacuolization; infiltration of inflammatory cells; and finally, the presence and/or deposition of different substances, such as interstitial myoglobin globules, lipofuscin pigment, polysaccharide complexes, and intra- and/or extravascular gas emboli and vessel dilation. This study advances our current knowledge about the histopathological findings in the cardiac muscle of cetaceans, and more specifically, of Cuvier's beaked whales.

Key words: cardiac lesions, Cuvier's beaked whales, histopathological findings, stranded cetaceans, stress cardiomyopathy

(Received 16 December 2021; revised 5 March 2022; accepted 5 April 2022)

Introduction

Histology is considered the assessment of the microscopic structures of animal and plant cells and characteristic tissues through staining, sectioning, and examining them under a microscope (electron or light microscope). Various methods are applied, with histological studies used extensively, not only in medicine for the study of diseased tissues to aid treatment but also in forensic investigations and/or autopsy (Alturkistani et al., 2015).

In humans, cardiac and vascular gross and microscopic anatomy has been appreciated for many years, which was followed by ultrastructural anatomy and physiology. However, pathogenesis was only clarified long after the disease was noted, and this realization is still humbling. For this reason, learning about both normal and abnormal heart function is an ongoing task (Buja & Butany, 2015).

Faced with this growing knowledge, the pathologist has become the data integrator, interpreting the clinical information, imaging, and finally, the gross and histopathological findings to make a clinically relevant diagnosis. Therefore, the pathologist must understand the normal cardiac anatomy before appreciating

pathology since the consideration of gross and microscopic anatomy allows the pathologist to understand the range of normal findings (Buja & Butany, 2015).

Cetacean hearts largely follow the gross general appearance found in other mammalian species, but they have some noteworthy differences. For example, the heart of dolphins is larger and flatter than that of most terrestrial mammals due to the shape of the thorax and the pressure it withstands. Therefore, it has an oval, almost circular outline, with wider (but shorter) ventricles, a slightly rotated axis, and auricles that are flat, with their ventral edges surpassing the coronary sulcus separating atria from ventricles. Histologically, the cardiac muscle in cetaceans is no different from that of terrestrial mammals. Cardiac muscle fibers (cardiomyocytes) are short, thinner than skeletal striated and uninucleated fibers, with the nucleus in the center of the cells. Three typical regions are distinguished: the epicardium, myocardium, and endocardium (Fernández et al., 2005*a*; Eurell & Frappier, 2013; Cozzi et al., 2017).

Considerable knowledge has been gained over the last few decades on several disease processes afflicting free-ranging cetaceans from a pathologist's point of view (Arbelo et al., 2013; Díaz-Delgado et al., 2018; Groch et al., 2018). For example, several studies have proven that deep-diving cetaceans, such as beaked whales, are threatened by anthropogenic activities. These include bycatch, debris ingestion, ship collisions, and any activity producing high-intensity noise (e.g., military sonars), which has even

CrossMark

been the cause of several unusual stranding events (Fernández et al., 2005*b*; Carrillo & Ritter, 2010; Virgili et al., 2019; Puig-Lozano et al., 2020). However, there is still a dearth of knowledge on cardiovascular lesions in these species, but, for the most part, the cardiac responses to different types of injury appear to follow similar patterns to those observed in humans and other animal species.

For this reason, this study aimed to partially fill in a gap of knowledge regarding histological findings in the cardiac muscle of free-ranging stranded cetaceans and, more specifically, of deep-diving Cuvier's beaked whales (*Ziphius cavirostris*).

Materials and Methods

One thousand, two hundred and ninety-nine cetaceans of 26 different species, including small and large odontocetes and mysticetes, were stranded on the coast of the Canary Islands from 1992 to 2020. Of these, 106 animals (8.16%) were initially included in this study and identified as being part of the Family *Ziphiidae* and were then categorized into the following species: Sowerby's beaked whales (*Mesoplodon bidens*) (3/106–2.83%), Blainville's beaked whales (*Mesoplodon densirostris*) (11/106–10.38%), Gervais' beaked whales (*Mesoplodon europaeus*) (16/106–15.09%), 1 True's beaked whale (*Mesoplodon mirus*) (1/106–0.94%), and Cuvier's beaked whale (*Ziphius cavirostris*) (73/106–68.87%). Since Cuvier's beaked whale was the species with the most individuals, we decided to focus our study exclusively on this species. A total of 49 out of the 73 animals (67.12%) were necropsied following the basic protocol for the performance of a cetacean necropsy outlined and published by the European Cetacean Society by Thijs Kuiken and Manuel García Hartmann (Proceedings of the first ECS workshop on Cetacean Pathology: Dissection Techniques and Tissue Sampling. Leiden, Netherlands, 13–14 September 1991. Newsletter # 17 special issue) (Kuiken & Hartmann, 1991). This protocol has undergone some modifications of the procedures referenced in the manual published by Geraci and Lounsbury in 2005 (Marine mammals ashore: a field guide for strandings), along with a more recent update and innovation by the European Cetacean Society by ASCOBANS and ACCOBAMS in 2019 (Proceedings of the ECS workshop on Cetacean Pathology: Necropsy Technique and Tissue Sampling. Funchal, Madeira, Portugal, April 2016). Tissue samples of approximately 2–3 cm^3 were collected during the necropsy and stored in 10% buffered formaldehyde for further histopathological analysis (Kuiken & Hartmann, 1991; Geraci & Lounsbury, 2005; ASCOBANS/ACCOBAMS, 2019). After being fixed for at least 24 h, the samples were cut (approximately 1.5 cm × 0.3 cm) and placed in cassettes for automatic processing and later inclusion in paraffin.

Thus, out of the initial 49 necropsied individuals we selected for our research, 15 animals (30.61%) presented very fresh, fresh, moderate, and advanced autolysis conservation states, which were also determined following the parameters and classifications established by this protocol (Kuiken & Hartmann, 1991; Geraci & Lounsbury, 2005; ASCOBANS/ACCOBAMS, 2019). Additionally, the pathological findings in the different organs and the causes of death were described in PhD theses, published as scientific articles, and presented in annual reports deliverable to the Government of the Canary Islands annually (Arbelo et al., 2013; Díaz-Delgado et al., 2018).

All the individuals (15–100%) were deceased when the stranding notification was received. Nevertheless, a total of six animals (40.00%) showed a clear evidence of being alive when stranded,

eight animals (53.33%) had no signs of live stranding, and the status of one animal (6.67%) was unclear.

Concerning the causes of death, the individuals died due to natural pathology associated with a good/moderate body condition (4/15–26.67%), natural pathology associated with a significant loss of body condition (3/15–20.00%), foreign-body ingestion pathology (3/15–20.00%), perinatal/neonatal pathology (2/15–13.33%), and ship strike (1/15–6.67%). It was impossible to determine the cause of death in two animals (13.33%).

The Veterinary Histology and Pathology Department of the Institute of Animal Health and Food Safety (IUSA) of the Veterinary School of the University of Las Palmas of Gran Canaria (ULPGC) is known at an international level. For this reason, on some occasions, the department acts as a consultant in specific cases. Consequently, different tissue samples of stranded cetaceans in different countries are also stored in the tissue bank of the department. As a result, we included a total of five Cuvier's beaked whales, that is, 4 (80.00%) stranded in Almería, Spain, in 2006 and 2011 and 1 (20.00%) stranded in Corfu, Greece, in 2011, which were part of atypical mass stranding (AMS) episodes and died due to gas embolism.

In conclusion, a total of 20 individuals were analyzed in this study.

All the cardiac tissue samples included in this study consisted mainly of left and/or right ventricles that were fixed and processed following standard histological procedures. Specifically, 4 μm thick sample sections were used for hematoxylin and eosin (HE) and periodic acid-Schiff staining, and 5 μm sections were used for phosphotungstic acid hematoxylin (PTAH) and Masson's trichrome techniques (Ovalle & Nahirney, 2008). The microscopic findings, identified during the cardiac examination under an optical microscope, were reviewed blindly by four veterinarians and/or pathologists (NC, ES, PH, and AF). The extent of the cardiac lesions was judged subjectively as follows: absent, mild, mild to moderate, moderate, moderate to severe, and severe.

The procedure described previously is summarized in Figure 1. Moreover, the basic epidemiological data and causes of death of the cetaceans included in this research are presented in Supplementary Table S1.

Results

The significant lesions described histologically in the cardiac muscle of the animals analyzed were (1) vascular changes (Supplementary Table S2), such as congestion, edema, hemorrhages, leukocytosis, and intravascular coagulation; (2) acute degenerative changes (Supplementary Table S3), which consisted of contraction band necrosis, wavy fibers, cytoplasmic hypereosinophilia, and perinuclear vacuolization; (3) infiltration of inflammatory cells (Supplementary Table S4); and (4) the presence and/or deposition of different substances (Supplementary Table S5), such as interstitial myoglobin globules, lipofuscin pigment, polysaccharide complexes, and intra- and/or extravascular gas emboli.

Regarding vascular changes, vascular congestion was observed in 13 out of the 20 animals (65.00%), and this phenomenon was identified by swelling and light occlusion of capillaries with blood. Eleven out of the 20 animals (55.00%) had interstitial edema, represented histologically by fibers separated by spaces. Hemorrhages, which consist of blood escaping from ruptured blood vessels, were identified in 5 out of the 20 animals (25.00%). These could be visualized in the endocardial, myocardial, and epicardial portions of the heart. Twelve out of the 20 animals (60.00%) presented leukocytosis and intravascular coagulation, which is a condition in which blood clots form and block
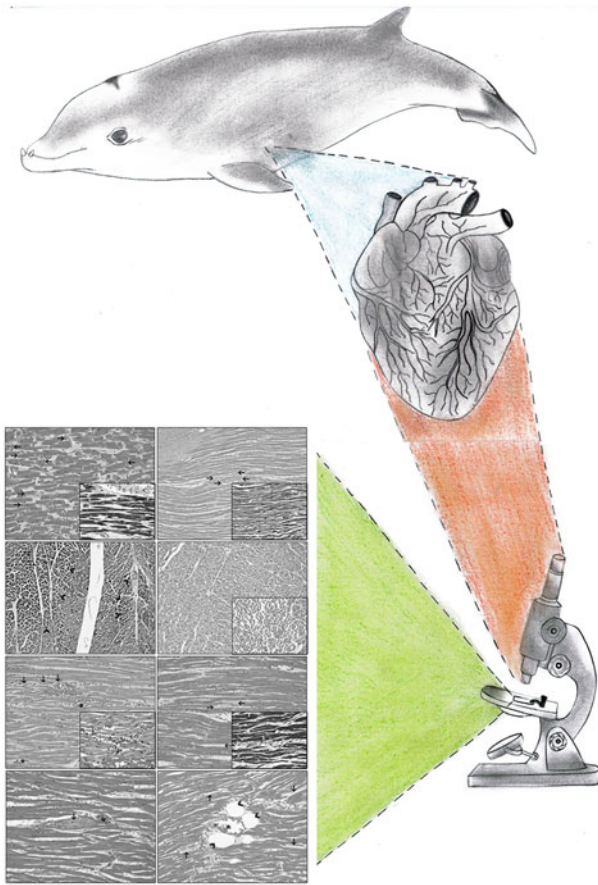
Fig. 1. This graphical abstract provides the readers with a visual representation of the conclusions and an efficient way to appreciate the work's critical findings and central message. This illustration describes the consecutive steps of the research, starting with the necropsy of stranded Cuvier's beaked whales (*Ziphius cavirostris*), in which a macroscopic assessment and sample collection of the cardiac muscle was performed. Then, the samples were processed employing a standard protocol for the blind evaluation of histological findings by veterinarians and/or pathologists using an optical microscope. Finally, the microscopical images resulting from the histological evaluation are used in the forthcoming figures of this article and the feature sizes may be seen from the micron markers in those later figures.

small blood vessels, together with the presence of inflammatory cells, more specifically, leukocytes.

Regarding acute degenerative changes, contraction band necrosis was observed in 8 out of the 20 animals (40.00%),

consisting of dense hypereosinophilic bands that ran transversely through the myocytes (Fig. 2). Fifteen out of the 20 animals (75.00%) exhibited long and thin undulated fibers, termed wavy fibers (Fig. 3). Hypereosinophilia was easily identified since the necrotic fibers presented more eosinophilic, blue, or red staining (using HE, PTAH, and Masson's trichrome techniques, respectively) than did adjacent normal fibers (Fig. 4). The above finding was detected in 15 out of the 20 animals (75.00%), being more pronounced in some cases at the subendocardial and subepicardial levels. Seventeen out of the 20 animals (85.00%) exhibited vacuolar degeneration (Fig. 5), morphologically characterized by the intracellular accumulation of fluid and the lysis of myofibrils. The liquid increase exerted pressure on the different parts of the cell, resulting in most of the fibers with vacuoles having a pyknotic nucleus, and in some cases, this lesion was more noticeable at both the subendocardial and the subepicardial levels.

In 9 out of the 20 animals (45.00%), different types of cells (Fig. 6) were identified as infiltrating zones where hemorrhages, fibrillary rupture of fibers, degeneration, and necrosis of cardiac cells were present. Of these, 3 out of the 20 animals (15.00%) displayed infiltration of mononuclear cells, another 4 out of the 20 animals (20.00%) presented infiltration by polymorphonuclear cells, and, finally, 5 out of the 20 animals (25.00%) exhibited infiltration of macrophages. It is also important to mention that 3 out of the 20 animals (15.00%) demonstrated infiltration with polymorphonuclear cells and macrophages.

Additionally, we verified the deposition of diverse substances, such as myoglobin, released by the ruptured cardiac fibers and accumulated as globules inside the blood vessels and in the interstitial spaces (Fig. 7). Myoglobin globules were observed in 14 out of the 20 animals (70.00%). Lipofuscin is one of the other substances that was detected in 5 out of the 20 animals (25.00%). It is a yellow–brown pigment resulting from the breakdown and absorption of damaged blood cells. In 4 out of the 20 animals (20.00%), polysaccharide complexes (Fig. 8) were present in the interior of the cardiomyocytes, defined as basophilic material inclusions. Vessel dilation and intra- and/or extravascular gas bubbles (Fig. 9), consisting of round empty spaces among the blood cells inside a vessel and/or the tissue cells inside the interstitium, were found in 7 out of the 20 animals (35.00%).

Discussion

Before entering a discussion of the results, the authors would like to emphasize that this research was conducted in stranded free-
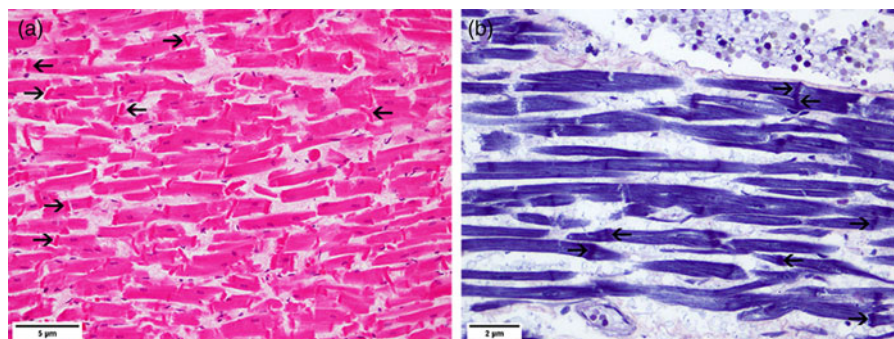

Fig. 2. (**a**) Animal 16 (ref: CET 771 – i414/15). Contraction band necrosis running (arrows) transversely through the cardiomyocytes and identified through the higher intensity of color with different histochemical techniques (in this case, with the HE technique). (**b**) Animal 10 (ref: CET 471 – i319/08). Details of the contraction band necrosis (arrows) analyzed with the PTAH technique.
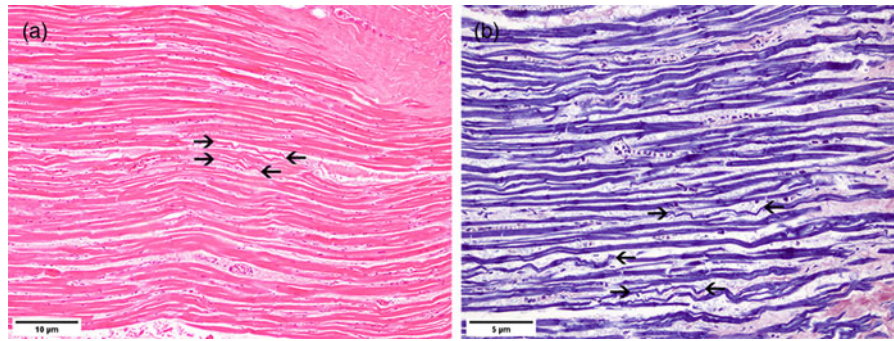
Fig. 3. (**a**) Animal 17 (ref: CET 855 – i197/17). Wavy fibers (arrows) consisting of long and thinned undulated fibers. HE technique. (**b**) Animal 17 (ref: CET 855 – i197/17). Details of the wavy fibers (arrows) analyzed with the PTAH technique.
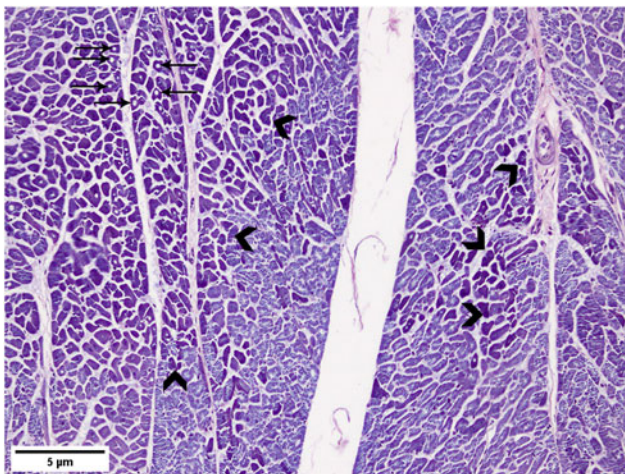

Fig. 4. Animal 15 (ref: CET 720 – i185/14). Hypereosinophilia consisting of increased staining of necrotic cardiac cells (arrowheads) with different techniques (in this case, with the PTAH technique). The presence of cytoplasmic vacuolization was observed in some injured cardiomyocytes (thin arrows).

ranging Cuvier's beaked whales. Since we are working with wild animals, stranding networks, and the general public, in a stranding event, it is often clinically and pathologically challenging to obtain the correct information and/or the complete history of each animal prior to its death (Arbelo et al., 2013; Díaz-Delgado et al., 2018). For this reason, the diagnosis of the pathological entity and/or cause of death, which may be

considered a complete puzzle, is based on the sum of the gross and/or histopathological findings or "puzzle pieces" identified during the pathological evaluation of the different organs. Nevertheless, it is essential to highlight that the observation of specific lesions may or may not be, direct or indirectly, associated with the cause of death. Therefore, the pathological entities and/or causes of death should be determined by an experienced veterinarian and/or pathologist (Arbelo et al., 2013; Díaz-Delgado et al., 2018).

In this investigation, the authors centered their attention exclusively on the histopathological findings of the hearts of stranded *Ziphius cavirostris*, which, in some cases, may be directly related to the cause of death.

Recent studies have characterized cardiac lesions associated with stressful situations, such as live stranding, ship collisions, and fishery interactions, as being comparable to the Stress Cardiomyopathy (SCMP) described in humans. These morphological alterations consist of vascular changes (i.e., congestion, interstitial edema, and hemorrhages) and acute degenerative lesions (i.e., contraction band necrosis, wavy fibers, hypereosinophilia, and cytoplasm vacuolization) with a perivascular distribution, indicative of ischemia–reperfusion damage. Additionally, infiltration of inflammatory cells, myoglobin globules and fibrotic tissue are also detected in this pathology (Herráez et al., 2007, 2013; Câmara et al., 2019a, 2019b, 2020a, 2020b; Puig-Lozano et al., 2020).

There is a chronological sequence in the changes of acute ischemic injuries, such as those described in SCMP syndrome, that were identified in this study; these changes can be observed as early as the first 5 min, starting with the presence of long,
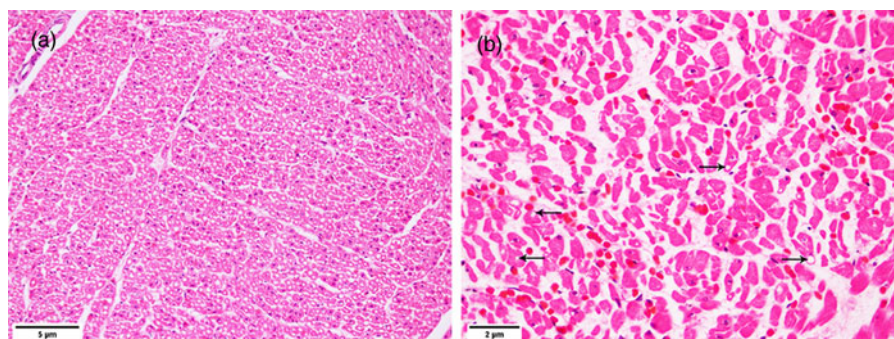

Fig. 5. (**a**) Animal 3 (ref: CET 236 – i34/04). Intracytoplasmic vacuoles (arrows) of cardiomyocytes identified with the HE technique. (**b**) Animal 1 (ref: CET 103-258/00). Vacuolar degeneration (arrows) in cardiac cells. HE.
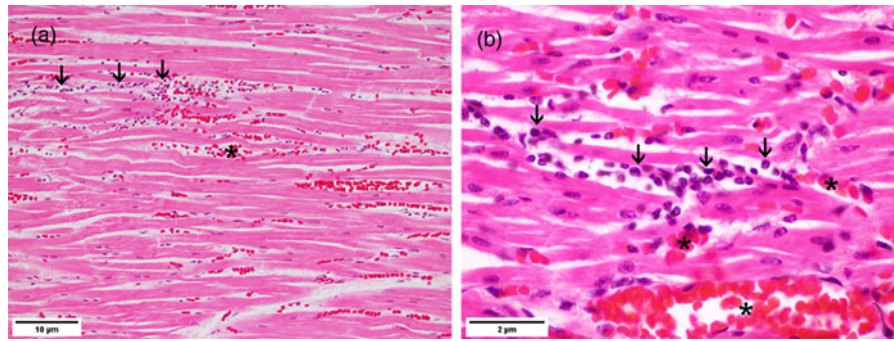
Fig. 6. (**a**) Animal 11 (ref: i76/11). The presence of inflammatory cells (arrows) in the interstitial space, with congestion (*). HE. (**b**) Animal 2 (ref: CET 113-384/00). Details of the infiltration of mononuclear cells (arrows) in a zone with ruptured cardiac fibers. Additionally, there is congestion (*) of the blood vessels. HE.
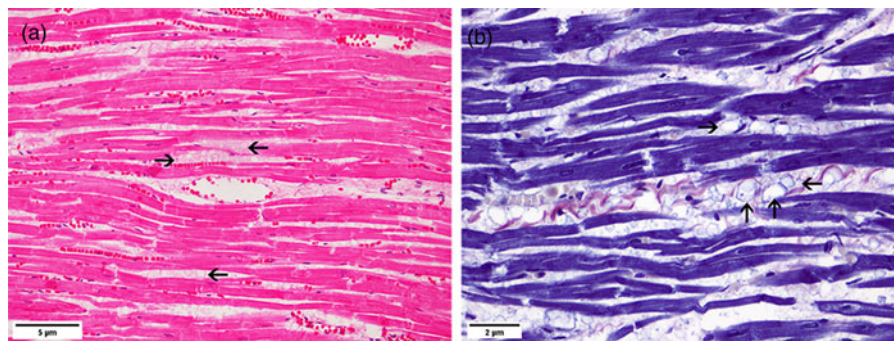

Fig. 7. (**a**) Animal 6 (ref: i17/06). Myoglobin globules (arrows) observed in the interstitial space. HE. (**b**) Animal 13 (ref: i384/11). Details of the myoglobin globules (arrows) stained with the PTAH technique.

thinned, wavy fibers (15/20–75.00%) separated by spaces representing edema (11/20–55.00%) and microvascular congestion (13/20–65.00%) at the borders of the ischemic myocardium. In the following 15 min, cell death may start to occur. Within 2 to 3 h, early changes in cardiomyocyte coagulation necrosis with nuclear pyknosis, color change, more specifically "red brick change" or cytoplasm hypereosinophilia (15/20–75.00%), focal contraction bands (8/20–40.00%) and subtle interstitial edema become evident. After 3 to 6 h, hypereosinophilia and edema become more pronounced and easily recognizable. Six to 12 h later, an increased number of neutrophils line up in capillaries, as well as accelerated changes and more extensive contraction band necrosis with reperfusion, become noticeable. In the next 12-h period and completing the 24-h cycle after the ischemic injury, extravazation into the interstitial space of neutrophils (4/20–20.00%) occurs, along with obvious vascular congestion,
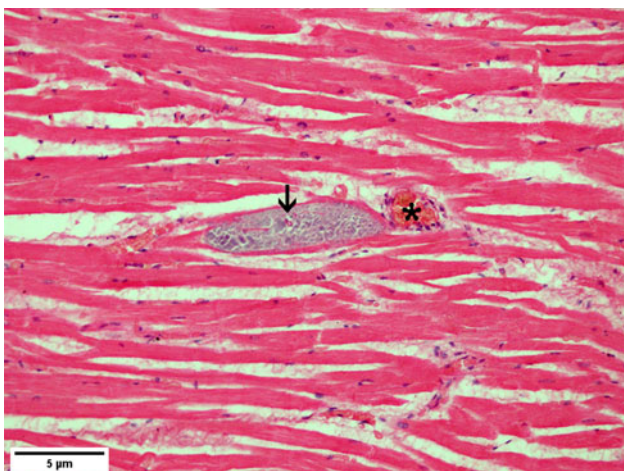

Fig. 8. Animal 6 (ref: i17/06). Basophilic material described as polysaccharide complexes (arrow) in the interior of the cardiomyocytes. Congestion (*) of the blood vessels is present. HE.
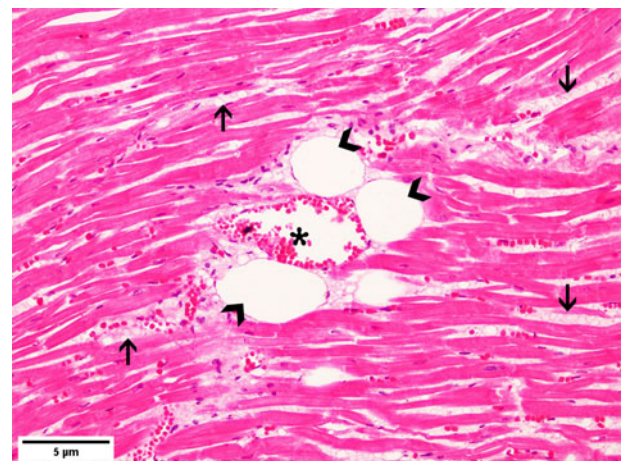

Fig. 9. Animal 6 (ref: i17/06). Round empty spaces compatible with extravascular gas bubbles (arrowheads) surrounding a blood vessel (*). Detection of myoglobin globules (arrows) in the interstitial space. HE.

interstitial edema, and focal areas of hemorrhage (5/20–25.00%). Subsequently, the subacute period starts.

A heavy influx of neutrophils is detected in the periphery, and lymphocytes (3/20–15.00%) start to appear at the edge of the infarction at 1 to 3 days. Degeneration of neutrophils becomes clear from 3 to 7 days, with basophilic granular debris produced as "nuclear dust". The beginning of the disintegration of necrotic myocytes with phagocytosis and removal of necrotic fibers, along with the evident presence of lymphocytes and the influx of macrophages (5/20–25.00%), is also observed.

Moreover, the onset of vascular and connective (granulation) tissue proliferation and early fibrosis has begun at the edge of the injury. Afterward, the chronic phase starts. After 2 weeks, chronic inflammation and the removal of peripheral muscle fibers occur, with increased numbers of mononuclear cells (macrophages) at the margins of the injury, where vascular and connective tissue proliferation has become more prominent. Eosinophils, lymphocytes, and plasma cells are also present, with infrequent neutrophils. Three to 4 weeks after ischemic injury, the continued removal of necrotic fibers and proliferation of granulation tissue extends throughout the injured area. Macrophages are still numerous, and plasma cells, eosinophils and lymphocytes are still present, but there is more substantial fibroblastic proliferation with collagen formation that is recognizable as a pink, fibrillary extracellular material. From 5 to 6 weeks, the removal of residual necrotic fibers and continued gradual scar formation with collagen deposition are identifiable. Inflammatory cells and vascularity decreases, but a few macrophages, plasma cells, and lymphocytes persist and remain in the scar that eventually forms. Finally, after 3 months, the fibrous scar is fully developed (Buja, 2005; Buja & Butany, 2015; Câmara et al., 2020a).

As mentioned before, these alterations have been associated with the cardiac pathology designated SCMP in cetaceans. Nevertheless, it is essential to highlight that these changes can sometimes imply a bias in the cases analyzed. For instance, some live-stranded animals tend to strand themselves due to previous pathological processes, such as infectious diseases, which are not always identifiable (Câmara et al., 2020a). Therefore, an example of this situation would be the animals that presented leukocytosis and intravascular coagulation (12/20–60.00%), which can be evaluated either as a case of disseminated intravascular coagulation (DIC) or as simply a phase of the acute ischemic injury described previously.

DIC is characterized by disseminated and often uncontrolled coagulation activation associated with a high risk of macro- and microvascular thrombosis and progressive consumption coagulopathy, which leads to an increased bleeding risk. Sepsis, cancer, trauma, and obstetric emergencies are ranked among the most frequent pathological conditions that may trigger DIC (Levi et al., 1993; Okajima, 1999; Okabayashi et al., 2004; Semeraro et al., 2010; Papageorgiou et al., 2018). The generalized Shwartzman reaction was the first sign demonstrating the relationship between leukocytes and coagulation abnormalities. Leukocytes have also been shown to have a crucial role in intravascular coagulation in patients with sepsis. Cytokines activate neutrophils, thus releasing various inflammatory mediators capable of damaging endothelial cells. This damage and thrombus formation may play a role in the development of organ failure in DIC associated with sepsis (Okajima, 1999).

Lipofuscin (5/20–25.00%) results from the accumulation of the end-product of intracellular lipid peroxidation or cellular metabolism during ageing (life stage) (Nakano et al., 1995). This pigment is widely observed in postmitotic cells, especially in long-lived cells such as neurons and cardiomyocytes. Therefore, lipofuscin is a pigment that accumulates during ageing (Kakimoto et al., 2019). To date, the pathogenic roles of lipofuscin have been strongly suggested in various diseases, such as the end stage of heart failure with dilated cardiomyopathy and ischemic cardiomyopathy (Rayment et al., 1999; Radu et al., 2012; Nozynski et al., 2013; Kakimoto et al., 2019).

Complex polysaccharide inclusions (4/20–20.00%) within skeletal muscle fibers occur in various human and animal disorders. In humans, such inclusions have been classified as incidental, age-related changes, such as in corpora amylacea in neural tissue or basophilic degeneration of the myocardium, and as pathological accumulations as a critical feature of the wide-ranging polyglucosan body disease (Cavanagh, 1999; Longué et al., 2020). Occasionally, these inclusions occur in skeletal or cardiac muscle in conditions such as Lafora body disease or as a primary lesion at sites of myopathies, including glycogen storage disorders (Cavanagh, 1999; Sierra et al., 2012; Hedberg-Oldfors & Oldfors, 2015; Longué et al., 2020). Similar inclusions have also been reported in animals and are most thoroughly studied in equine polysaccharide storage myopathy (Valentine et al., 1997; Sierra et al., 2012; Longué et al., 2020). In cetaceans, these intramyofiber Pas-positive, diastase-resistant aggregates and granules have already been described as present within the skeletal muscles of several cetacean species and within the myocardium of pilot whales. Nevertheless, the pathogenesis and clinical significance remain undetermined (Scotti, 1962; Cowan, 1966; Sierra et al., 2012; Longué et al., 2020).

The formation of intravascular and extravascular gas bubbles (7/20–35.00%) are the main findings of forensic investigations related to a widely known clinical syndrome in human medicine, mainly occurring in divers, called Decompression Sickness (Vann et al., 2011; Velázquez-Wallraf et al., 2021). Gas embolism and decompression-like sickness have also been described in wild animals, first in cetaceans, more specifically with mass strandings of beaked whales, which occurred in 2003 and were coincidental in time and space with naval maneuvres (Jepson et al., 2003). Since then, many other cases have been diagnosed in cetaceans and other species, such as turtles (Fernández et al., 2005b, 2017; García-Párraga et al., 2014). More recently, the decompressive pathology in cetaceans has been studied through an experimental pathological model, where the presence of not only gas bubbles but also other gross and histological lesions, such as vascular changes (e.g., interstitial edema, hemorrhages) and/or acute degenerative changes (e.g., contraction band necrosis, wavy fibers, hypereosinophilia, intracytoplasmic vacuolization), was described (Velázquez-Wallraf et al., 2021). Although these changes have been reported in previous investigations, it is essential to remark that in our study, there was no apparent difference and/or relationship between the extension and severity of the acute degenerative lesions and the atypical mass stranding involving beaked whales with gas embolism when compared with the corresponding findings related to other causes of death, such as live stranding or ship collision, with a stress component associated in both deep- and shallow-diving cetaceans.

Summary or Conclusion

Herein, we present the prevalence and types of cardiac histopathological findings in stranded free-ranging Cuvier's beaked whales. Although some of these observed features were considered

incidental or of little clinical and/or pathological relevance, others could have resulted in severe cardiovascular dysfunction, such as those injuries compatible with the damage occurring with the SCMP described in humans and cetaceans. In conclusion, these results advance our understanding of cetacean pathology, may prove to be of value to diagnosticians, and may guide future comparative pathologic studies, which can improve our medical and conservation efforts by reducing the mortality of these animals.

Availability of data and material

All data reported in this work are classified and stored in the tissue bank of the Veterinary Histology and Pathology Department of the Institute of Animal Health and Food Safety (IUSA) of the Veterinary School of the University of Las Palmas of Gran Canaria (ULPGC) (Campus Universitario Cardones de Arucas, Trasmontaña s/n, 35413 Arucas, Las Palmas of Gran Canaria, Spain).

References

Alturkistani HA, Tashkandi FM & Mohammedsaleh ZM (2015). Histological stains: A literature review and case study. *Glob J Health Sci* **8**, 72–79.

Arbelo M, Monteros AEDL, Herráez P, Andrada M, Sierra E, Rodríguez F, Jepson PD & Fernández A (2013). Pathology and causes of death of stranded cetaceans in the Canary Islands (1999–2005). *Dis Aquat Org* **103**, 87–99.

ASCOBANS/ACCOBAMS (2019). *European Best Practice on Cetacean Post-Mortem Investigation and Tissue Sampling*. OSFPREPRINTS.

Buja LM (2005). Myocardial ischemia and reperfusion injury. *Cardiovasc Pathol* **14**, 170–175.

Buja LM & Butany J (2015). *Cardiovascular Pathology*. London, UK: Elsevier Science.

Câmara N, Sierra E, Fernández A, Arbelo M, Andrada M, Monteros AEDL & Herráez P (2020*a*). Increased plasma cardiac troponin I in live-stranded cetaceans: Correlation with pathological findings of acute cardiac injury. *Sci Rep* **10**, 1555.

Câmara N, Sierra E, Fernández A, Arbelo M, Bernaldo de Quirós Y, Arregui M, Consoli F & Herráez P (2020*b*). Capture myopathy and stress cardiomyopathy in a live-stranded Risso's dolphin (*Grampus griseus*) in rehabilitation. *Animals* **10**, 220.

Câmara N, Sierra E, Fernández A, Suárez-Santana CM, Puig-Lozano R, Arbelo M & Herráez P (2019*b*). Skeletal and cardiac rhabdomyolysis in a live-stranded neonatal Bryde's whale with fetal distress. *Front Vet Sci* **6**, 476–476.

Câmara N, Sierra E, Fernández-Maldonado C, Monteros AEDL, Arbelo M, Fernández A & Herráez P (2019*a*). Stress cardiomyopathy in stranded cetaceans: A histological, histochemical and immunohistochemical study. *Vet Rec* **185**, 694.

Carrillo M & Ritter F (2010). Increasing numbers of ship strikes in the canary islands: Proposals for immediate action to reduce risk of vessel-whale collisions. *J Cetacean Res Manage* **11**, 131–138.

Cavanagh JB (1999). Corpora-amylacea and the family of polyglucosan diseases. *Brain Res Rev* **29**, 265–295.

Cowan DF (1966). Pathology of the pilot whale. *Globicephala melaena*. A comparative survey. *Arch Pathol* **82**, 178–189.

Cozzi B, Huggenberger S & Oelschläger H (2017). *Anatomy of Dolphins: Insights into Body Structure and Function*. Amsterdam: Elsevier, Academic Press.

Díaz-Delgado J, Fernández A, Sierra E, Sacchini S, Andrada M, Vela AI, Quesada-Canales Ó, Paz Y, Zucca D, Groch K & Arbelo M (2018). Pathologic findings and causes of death of stranded cetaceans in the Canary Islands (2006–2012). *PLoS One* **13**, e0204444.

Eurell JA & Frappier BL (2013). *Dellmann's Textbook of Veterinary Histology*. Iowa, USA: John Wiley & Sons.

Fernández A, Caballero MJ & Jaber JR (2005*a*). *Atlas de Histología de Peces y Cetáceos*. Las Palmas de Gran Canaria: Servicio de Publicaciones y Difusión Científica de la ULPGC.

Fernández A, Edwards JF, Rodríguez F, Monteros AEDL, Herráez P, Castro P, Jaber JR, Martín V & Arbelo M (2005*b*). "Gas and fat embolic syndrome" involving a mass stranding of beaked whales (family Ziphiidae) exposed to anthropogenic sonar signals. *Vet Pathol* **42**, 446–457.

Fernández A, Sierra E, Díaz-Delgado J, Sacchini S, Sánchez-Paz Y, Suárez-Santana C, Arregui M, Arbelo M & Quirós YBD (2017). Deadly acute decompression sickness in Risso's dolphins. *Sci Rep* **7**, 13621.

García-Párraga D, Crespo-Picazo JL, de Quirós YB, Cervera V, Martí-Bonmati L, Díaz-Delgado J, Arbelo M, Moore MJ, Jepson PD & Fernández A (2014). Decompression sickness ('the bends') in sea turtles. *Dis Aquat Org* **111**, 191–205.

Geraci JR & Lounsbury VJ (2005). *Marine Mammals Ashore: A Field Guide for Strandings*. Baltimore, MD: National Aquarium in Baltimore.

Groch KR, Díaz-Delgado J, Marcondes MCC, Colosio AC, Santos-Neto EB, Carvalho VL, Boos GS, Meirelles ACOD, Ramos HGDC, Guimarães JP, Borges JCG, Vergara-Parente JE, St Leger JA, Fernández A & Catão-Dias JL (2018). Pathology and causes of death in stranded humpback whales (*Megaptera novaeangliae*) from Brazil. *PLoS One* **13**, e0194872.

Hedberg-Oldfors C & Oldfors A (2015). Polyglucosan storage myopathies. *Mol Aspects Med* **46**, 85–100.

Herráez P, Espinosa de los Monteros A, Fernández A, Edwards JF, Sacchini S & Sierra E (2013). Capture myopathy in live-stranded cetaceans. *Vet J* **196**, 181–188.

Herráez P, Sierra E, Arbelo M, Jaber JR, Monteros AEDL & Fernández A (2007). Rhabdomyolysis and myoglobinuric nephrosis (capture myopathy) in a striped dolphin. *J Wildl Dis* **43**, 770–774.

Jepson PD, Arbelo M, Deaville R, Patterson IAP, Castro P, Baker JR, Degollada E, Ross HM, Herráez P, Pocknell AM, Rodríguez F, Howie FE, Espinosa A, Reid RJ, Jaber JR, Martin V, Cunningham AA & Fernández A (2003). Gas-bubble lesions in stranded cetaceans. *Nature* **425**, 575–576.

Kakimoto Y, Okada C, Kawabe N, Sasaki A, Tsukamoto H, Nagao R & Osawa M (2019). Myocardial lipofuscin accumulation in ageing and sudden cardiac death. *Sci Rep* **9**, 3304.

Kuiken T & Hartmann MG (1991). Dissection techniques and tissue sampling. European cetacean society newsletter, 17 (special issue). In *Proceeding of the First ECS Workshop on Ceacean Pathology Leiden, The Netherlands*. Stralsund: European Cetacean Society.

Levi M, Cate HT, van der Poll T & van Deventer SJ (1993). Pathogenesis of disseminated intravascular coagulation in sepsis. *JAMA* **270**, 975–979.

Longué CM, Dagleish MP, McGovern G, Brownlow AC & Baily JL (2020). Intrasarcoplasmic polyglucosan inclusions in heart and skeletal muscles of long-finned pilot whales (*Globicephala melas*) may be age-related. *J Comp Pathol* **181**, 18–25.

Nakano M, Oenzil F, Mizuno T & Gotoh S (1995). Age-related changes in the lipofuscin accumulation of brain and heart. *Gerontology* **41**, 69–80.

Nozynski J, Zakliczynski M, Konecka-Mrowka D, Zakliczynska H, Pijet M, Zembala-Nozynska E, Lange D & Zembala M (2013). Advanced glycation end products and lipofuscin deposits share the same location in cardiocytes of the failing heart. *Exp Gerontol* **48**, 223–228.

Okabayashi K, Wada H, Ohta S, Shiku H, Nobori T & Maruyama K (2004). Hemostatic markers and the sepsis-related organ failure assessment score in patients with disseminated intravascular coagulation in an intensive care unit. *Am J Hematol* **76**, 225–229.

Okajima K (1999). The role of leukocytes in disseminated intravascular coagulation associated with sepsis. *Sepsis* **3**, 135–142.

Ovalle WK & Nahirney PC (2008). *Netter Bases da Histologia*. Rio de Janeiro: Elsevier Brasil.

Papageorgiou C, Jourdi G, Adjambri E, Walborn A, Patel P, Fareed J, Elalamy I, Hoppensteadt D & Gerotziafas GT (2018). Disseminated intravascular coagulation: An update on pathogenesis, diagnosis, and therapeutic strategies. *Clin Appl Thromb/Hemostasis* **24**, 8S–28S.

Puig-Lozano R, Fernández A, Sierra E, Saavedra P, Suárez-Santana CM, Fuente JDL, Díaz-Delgado J, Godinho A, García-Álvarez N, Zucca D, Xuriach A, Arregui M, Felipe-Jiménez I, Consoli F, Díaz-Santana PJ, Segura-Göthlin S, Câmara N, Rivero MA, Sacchini S, Bernaldo de Quirós Y & Arbelo M (2020). Retrospective study of fishery interactions in stranded cetaceans, Canary Islands. *Front Vet Sci* **7**, 567258.

Radu RI, Bold A, Pop OT, Mălăescu DG, Gheorghişor I & Mogoantă L (2012). Histological and immunohistochemical changes of the myocardium in dilated cardiomyopathy. *Rom J Morphol Embryol* **53**, 269–275.

Rayment NB, Haven AJ, Madden B, Murday A, Trickey R, Shipley M, Davies MJ & Katz DR (1999). Myocyte loss in chronic heart failure. *J Pathol* **188**, 213–219.

Scotti TM (1962). Basophilic degeneration of the myocardium in a whale and a horse. *Am J Clin Pathol* **38**, 530–532.

Semeraro N, Ammollo CT, Semeraro F & Colucci M (2010). Sepsis-associated disseminated intravascular coagulation and thromboembolic disease. *Mediterr J Hematol Infect Dis* **2**, e2010024.

Sierra E, Fernández A, Monteros AEDL, Jaber JR, Andrada M & Herráez P (2012). Complex polysaccharide inclusions in the skeletal muscle of stranded cetaceans. *Vet J* **193**, 152–156.

Valentine BA, Credille KM, Lavoie JP, Fatone S, Guard C, Cummings JF & Cooper BJ (1997). Severe polysaccharide storage myopathy in Belgian and Percheron draught horses. *Equine Vet J* **29**, 220–225.

Vann RD, Butler FK, Mitchell SJ & Moon RE (2011). Decompression illness. *Lancet* **377**, 153–164.

Velázquez-Wallraf A, Fernández A, Caballero MJ, Møllerløkken A, Jepson PD, Andrada M & Quirós YBD (2021). Decompressive pathology in cetaceans based on an experimental pathological model. *Front Vet Sci* **8**, 676499.

Virgili A, Authier M, Boisseau O, Cañadas A, Claridge D, Cole T, Corkeron P, Dorémus G, David L, Di-Méglio N, Dunn C, Dunn TE, García-Barón I, Laran S, Lauriano G, Lewis M, Louzao M, Mannocci L, Martínez-Cedeira J, Palka D, Panigada S, Pettex E, Roberts JJ, Ruiz L, Saavedra C, Santos MB, Van Canneyt O, Bonales JAV, Monestiez P & Ridoux V (2019). Combining multiple visual surveys to model the habitat of deep-diving cetaceans at the basin scale. *Glob Ecol Biogeogr* **28**, 300–314.